ORIGINAL PAPER

Cr(II) and Cr(III) NCN pincer complexes: synthesis, structure, and catalytic reactivity

Matthias G. Käfer[1] · Wolfgang Eder[1] · Jan Pecak[1] · Berthold Stöger[2] · Marc Pignitter[3] · Luis F. Veiros[4] · Karl Kirchner[1]

Abstract

The synthesis, characterization, and reactivity of several new Cr(II) and Cr(III) complexes featuring an NCN pincer ligand with an arene backbone connected to amine donors NEt$_2$ and NiPr$_2$ via CH$_2$-linkers is described. Reacting the in situ lithiated ligand precursor N(C–Br)N^{CH2}-Et with [CrCl$_3$(THF)$_3$] resulted in the formation of the Cr(III) complex *trans*-[Cr(κ^3*NCN*-NCN^{CH2}-Et)(Cl)$_2$(THF)]. Upon reaction of lithiated N(C–Br)N^{CH2}-*i*Pr with a suspension of anhydrous CrCl$_2$, the Cr(II) complex [Cr(κ^2*NC*-NCN^{CH2}-*i*Pr)$_2$] is formed featuring two NCN ligands bound in κ^2*NC*-fashion. In contrast, when lithiated N(C–Br)N^{CH2}-*i*Pr is reacted with a homogeneous solution of anhydrous CrX_2 (X = Cl, Br), complexes [Cr(κ^3*NCN*-NCN^{CH2}-*i*Pr)X] are obtained. Treatment of [Cr(κ^3*NCN*-NCN^{CH2}-*i*Pr)Cl] with 1 equiv of PhCH$_2$MgCl and LiCH$_2$SiMe$_3$ afforded the alkyl complexes [Cr(κ^3*NCN*-NCN^{CH2}-*i*Pr)(CH$_2$Ph)] and [Cr(κ^3*NCN*-NCN^{CH2}-*i*Pr)(CH$_2$SiMe$_3$)]. All Cr(II) complexes exhibit effective magnetic moments in the range of 4.7–4.9 μ_B which is indicative for d^4 high spin systems. If a solution of lithiated N(C–Br)N^{CH2}-*i*Pr is treated with CrCl$_2$, followed by addition of an excess of Na[HB(Et)$_3$], the dimeric complex [Cr(κ^2*NC*-NCN^{CH2}-*i*Pr)(μ_2-H)]$_2$ is obtained bearing two bridging hydride ligands. [Cr(κ^3*NCN*-NCN^{CH2}-*i*Pr)(CH$_2$SiMe$_3$)] turned out to be catalytically active for the hydrosilylation of ketones at room temperature with a catalyst loading of 1 mol%. X-ray structures of all complexes are presented.

Graphical abstract
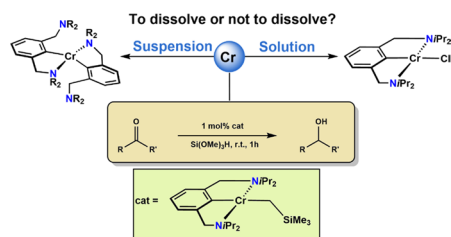
✉ Karl Kirchner
karl.kirchner@tuwien.ac.at

1 Institute of Applied Synthetic Chemistry, TU Wien, Getreidemarkt 9/163-AC, 1060 Vienna, Austria

2 X-Ray Center, TU Wien, Getreidemarkt 9/163-AC, 1060 Vienna, Austria

3 Department of Physiological Chemistry, Faculty of Chemistry, University of Vienna, Althanstraße 14, 1090 Vienna, Austria

4 Centro de Química Estrutural, Institute of Molecular Sciences, Departamento de Engenharia Química, Instituto Superior Técnico, Universidade de Lisboa, Av. Rovisco Pais, 1049 001 Lisbon, Portugal

Scheme 1
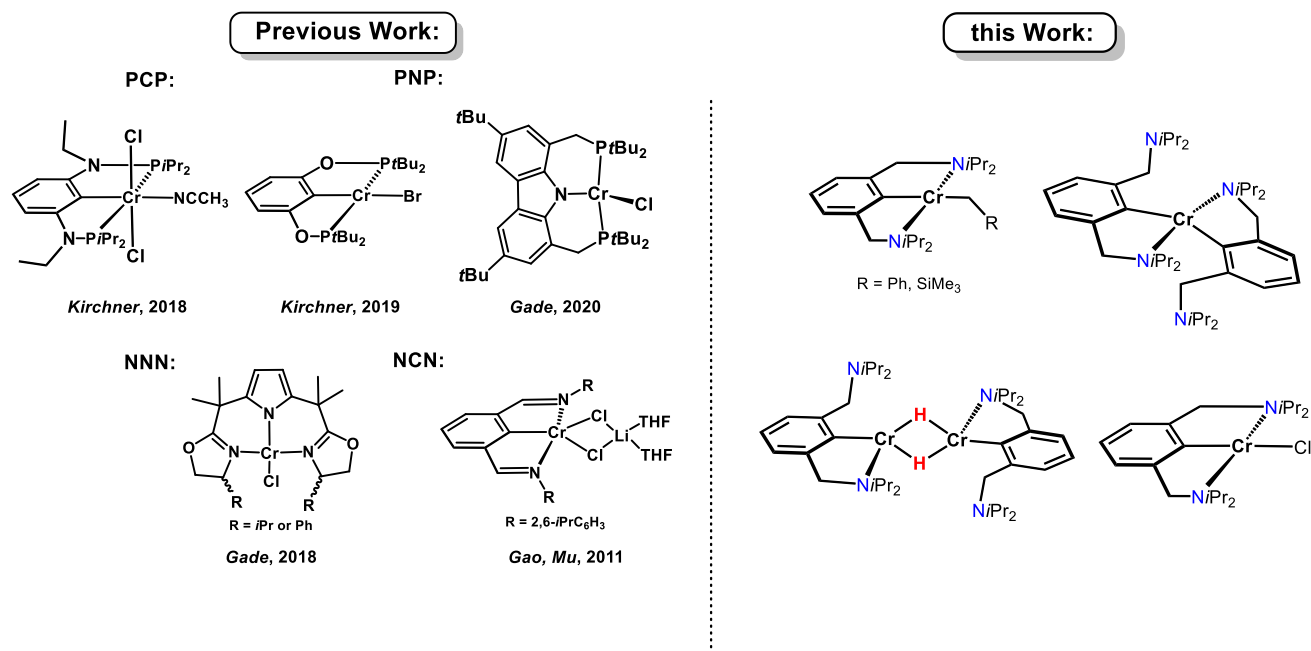
Introduction

In contrast to the chemistry of transition metal PCP pincer complexes [1–12] which feature an aromatic anionic arene backbone connected to phosphine donors via various linkers (CH$_2$, O, NH, NR), the chemistry of NCN pincer complexes featuring amine donors instead is rich but largely limited to Ni, Pd, and Pt [13–19]. Most notably, van Koten and coworkers prepared numerous Pd and Pt complexes for applications in catalysis, sensor systems, or even as building blocks for biomolecular and peptide chemistry. The major difference affecting the coordination chemistry of NCN ligands is that the N-atom is significantly smaller than the corresponding P-atom in PCP ligands and the aliphatic NR$_2$ group acts exclusively as a σ-donor. Moreover, NCN ligands are coordinated typically in planar tridentate *mer*-fashion, but in some cases also a *fac* geometry was observed [19].

Expanding on previous work with cobalt NCN pincer complexes [20] we envisioned a further contribution to the virtually non-existing field of chromium NCN pincer chemistry. It has to be noted that some Cr(III), Cr(II), and Cr(I)) PCP pincer complexes were reported recently [21–23]. Moreover, Cr(II) complexes containing monoanionic PNP and NNN-pincer type ligands featuring a pyrrole backbone were reported by Gade and coworkers (Scheme 1) [24, 25]. Gao, et al. [26] described the synthesis of Cr(III) bis(imino) aryl NCN pincer complexes which were applied as catalysts for isoprene polymerization.

Herein we report on the synthesis, characterization, and reactivity of several new Cr(II) and Cr(III) complexes featuring an NCN pincer-ligand with an arene backbone connected to amine donors NEt$_2$ and NiPr$_2$ via CH$_2$-linkers. Representative X-ray structures, EPR-spectra, and DFT calculations are presented.

Results and discussion

The in situ lithiation of N(C–Br)N^{CH2}-Et (1) with *n*-BuLi in THF at − 90 °C followed by addition of [CrCl$_3$(THF)$_3$] resulted, after workup, in the formation of complex *trans*-[Cr(κ^3*NCN*-NCN^{CH2}-Et)(Cl)$_2$(THF)] (3) in isolated 63% yield (Scheme 2). The measurement of the solution magnetic properties (Evans method, benzene [27]) revealed an effective magnetic moment of 3.7(2) μ_B which is consistent with three unpaired electrons as expected for a d^3 configuration and an oxidation state of + III. Figure 1 depicts the EPR spectrum of 3 obtained from a frozen toluene solution at 100 K, which confirms the expected quartet ground state. This spectrum has been successfully simulated

Scheme 2
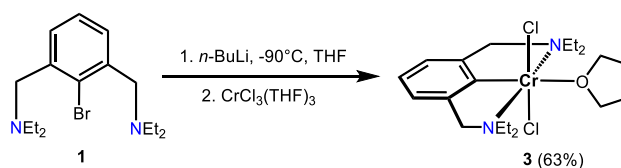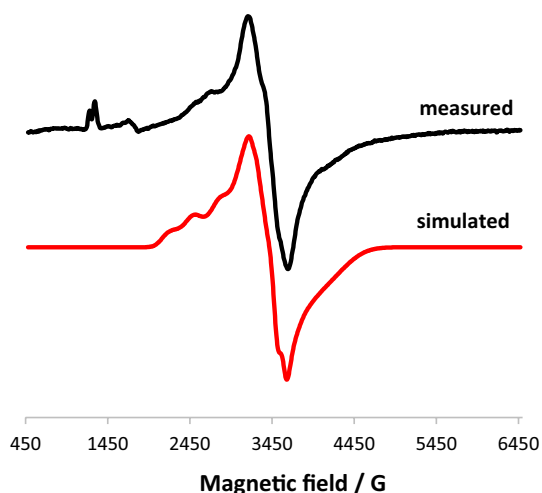
Fig. 1 X-band EPR spectrum at a microwave frequency of 9.86 GHz of $[Cr(\kappa^3 NCN\text{-}NCN^{CH2}\text{-}Et)(Cl)_2(THF)]$ (**3**) in frozen toluene glass at 100 K
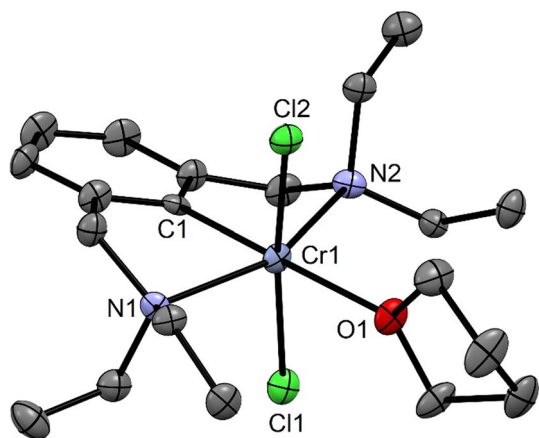
Fig. 2 Structural views of *trans*-$[Cr(\kappa^3 NCN\text{-}NCN^{CH2}\text{-}Et)(Cl)_2(THF)]$ (**3**) showing 50% thermal ellipsoids (H atoms are omitted for clarity). Selected bond lengths (Å) and bond angles (°): Cr1–C1 1.995(7), Cr1–N1 2.294(7), Cr1–N2 2.293(7), Cr1–Cl1 2.377(3), Cr1–Cl2 2.377(3), Cr1–O1 2.245(6), C20–Cr1–O1 179.5(4), N2–Cr1–N1 155.1(3), Cl2–Cr1–Cl1 171.82(9)

using the following parameters: $g_x = 1.989$, $g_y = 1.764$, g_z 2.392 ($g_{iso} = 2.048$) and ^{53}Cr hyperfine coupling constants $A_{x,1} = 82.575$, $A_{y,1} = 0.009$, $A_{z,1} = 315.588$ and $A_{x,2} = 19.677$, $A_{y,2} = 251.114$ and $A_{z,2} = 107.022$. The observed effective g_{iso}-value is typical for an electronic spin of $S = 3/2$.

To unequivocally establish the ligand arrangement and geometry, single crystals were grown by slow diffusion of *n*-pentane into a saturated THF at room temperature. A view of the molecular structure is depicted in Fig. 2 with selected metrical parameters reported in captions. The complex adopts a distorted octahedral geometry. While the C1–Cr1–O1 and Cl1–Cr1–Cl2 angles deviate only

Scheme 3
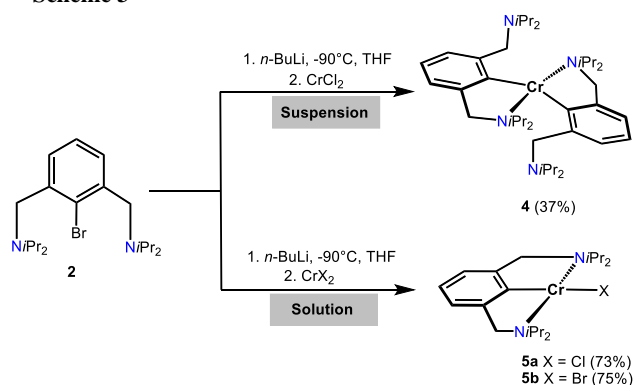
slightly from linearity being 179.5(4)° and 171.5(4)°, respectively, whereas the N1–Cr1–N2 angle deviate significantly from 180° being 155.1(3)°. Similar geometries were recently found for the analogous complexes *trans*-$[Cr(\kappa^3 PCP\text{-}POCOP\text{-}iPr)(Br)_2(THF)]$, *trans*-$[Cr(\kappa^3 PCP\text{-}PCP^{NEt}\text{-}iPr)(Cl)_2(THF)]$, and *trans*-$[Cr(\kappa^3 PCP\text{-}PCP^{CH2}\text{-}iPr)(Br)_2(CH_3CN)]$ [21, 23]. The Cr–C_{ipso} distance is 1.995(7) Å being comparable to those of other Cr(III) PCP pincer complexes. The Cr–C_{ipso} bond distance in $[Cr(\kappa^3 PCP\text{-}POCOP\text{-}tBu)(Br)]$, *trans*-$[Cr(\kappa^3 PCP\text{-}POCOP\text{-}iPr)(Br)_2(THF)]$, $[Cr(\kappa^3 PCP\text{-}POCOP\text{-}tBu)(\kappa^2\text{-}BH_4)]$, $[Cr(\kappa^3 PCP\text{-}POCOP\text{-}tBu)(NO)(\kappa^2\text{-}BH_4)]$, $[Cr(\kappa^3 PCP\text{-}POCOP\text{-}tBu)(NO)(Br)]$ [22], and *trans*-$[Cr(\kappa^3 PCP\text{-}PCP^{CH2}\text{-}iPr)(Br)_2(CH_3CN)]$ [23] are 2.084(3), 2.067(5), 2.076(2), 2.068(3), 2.056(2), and 2.052(1) Å, respectively.

Treatment of lithiated N(C–Br)N^{CH2}-Et (**1**) with anhydrous CrCl$_2$ resulted in the formation of intractable paramagnetic products. Gratifyingly, the reaction of the bulkier ligand N(C–Br)N^{CH2}-*i*Pr (**2**) with a suspension of anhydrous CrCl$_2$ under otherwise similar reaction conditions afforded, after workup, $[Cr(\kappa^2 NC\text{-}NCN^{CH2}\text{-}iPr)_2]$ (**4**) in 37% isolated yield (Scheme 3). This complex contains two NCN ligands bound in $\kappa^2 NC$-fashion. Evaluation of the solution magnetic properties of **4** (Evans method, benzene) showed an effective magnetic moment of 4.7(3) μ_B which is indicative for a d^4 high spin system featuring four unpaired electrons.

Cooling of a saturated *n*-pentane solution of **4** to −30 °C led to the formation of crystals suitable for single-crystal X-ray diffraction studies. A structural view of **4** is depicted in Fig. 3 with selected bond distances and angles given in the caption. Complex **4** adopts a strongly distorted tetrahedral coordination geometry as also seen from the structural parameters τ_4 and τ_4' being 0.51 and 0.50, respectively ($\tau_4 = \tau_4' = 0$ indicates an ideal square planar structure, $\tau_4 = \tau_4' = 1$ indicates an ideal tetrahedral structure and a $\tau_4 \approx 0.43$ and $\tau_4' \approx 0.24$ represents a seesaw geometry) [28]. The NCN ligand is coordinated in $\kappa^2 NC$-fashion and features one pendant amine arm.
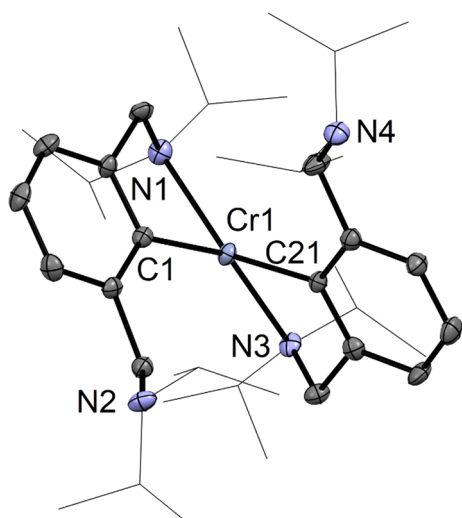
Fig. 3 Crystal structure of [Cr(κ^2NC-NCN^{CH2}-iPr)$_2$] (**4**) with 50% thermal ellipsoids (H-atoms omitted for clarity). Selected bond lengths (Å) and bond angles (°): Cr1-C1 2.073(4), Cr-C21 2.090(4), Cr1-N1 2.381(4), Cr-N3 2.371(4), C1-Cr1-N3 145.0(1), C21-Cr1-N1 143.7(2)
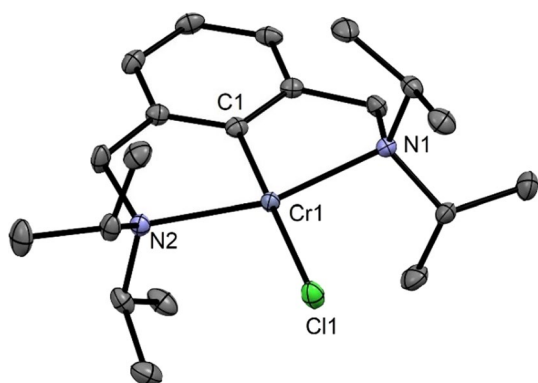
Fig. 4 Crystal structure of [Cr(κ^3NCN-NCN^{CH2}-iPr)Cl] (**5a**) with 50% thermal ellipsoids (H-atoms omitted for clarity). Selected bond lengths (Å) and bond angles (°): Cr1-C1 2.011(2), Cr1-N1 2.261(2), Cr1-N2 2.257(2), Cr-Cl1 2.4546(6), C1-Cr1-Cl1 178.59(7), N1-Cr1-N2 158.52(8)
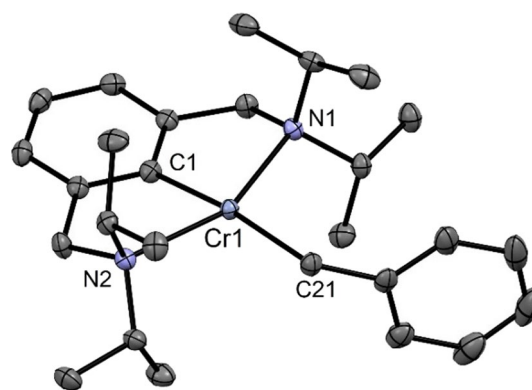

Fig. 5 Crystal structure of [Cr(κ^3NCN-NCN^{CH2}-iPr)(CH$_2$Ph)] (**6**) with 50% thermal ellipsoids (H-atoms omitted for clarity). Selected bond lengths (Å) and bond angles (°): Cr1-C1 2.043(1), Cr1-N1 2.291(1), Cr1-N2 2.327(1), Cr1-C21 2.249(1), C1-Cr1-C21 173.29(5), N1-Cr1-N2 154.99(4)

In contrast, when the lithiated ligand N(C–Br)N^{CH2}-iPr (**2**) is reacted with a solution rather than a suspension of anhydrous CrCl$_2$ or CrBr$_2$ in THF, obtained after ultrasonic irradiation, complexes [Cr(κ^3NCN-NCN^{CH2}-iPr)Cl] (**5a**) and [Cr(κ^3NCN-NCN^{CH2}-iPr)Br] (**5b**) were obtained in 73 and 75% isolated yields (Scheme 3). As indicated by solution magnetic susceptibility measurements (Evans method, benzene), these compounds are high-spin complexes with a solution-effective magnetic moment of 4.8(2) and 4.7(2) μ_B. This is in agreement with a high-spin d^4 center (four unpaired electron) and is in the same range as the theoretical spin-only value of 4.90 μ_B.

The molecular structure of **5a** shows the metal in a typical distorted-square planar configuration ($\tau_4 = 0.16$, $\tau_4' = 0.10$) [27]. The C1–Cr1–Cl1 angle deviates slightly from linearity 178.59(7)°. The N1–Cr1–N2 angle is 158.52(8)°. The Cr–C$_{ipso}$ bond distance of 2.011(2) Å is comparable to those of other Cr(II) pincer complexes [22] (Fig. 4)

Treatment of **5a** with 1 equiv of PhCH$_2$MgCl and LiCH$_2$SiMe$_3$ in toluene for 1.5 h afforded the alkyl

Scheme 4
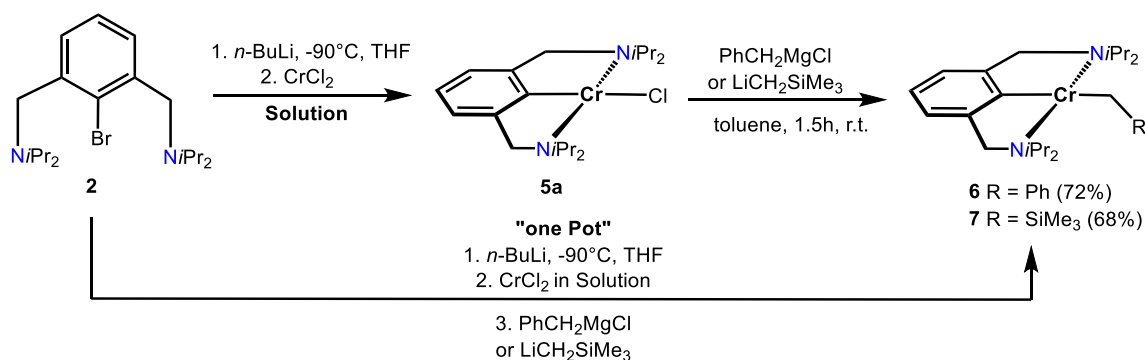
Scheme 5
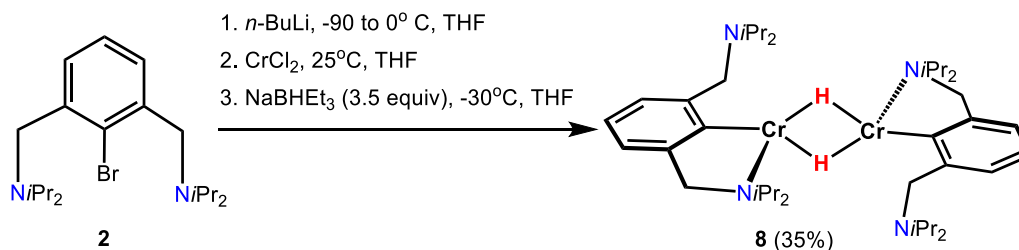
complexes [Cr(κ^3*NCN*-NCN^{CH2}-*i*Pr)(CH$_2$Ph)] (**6**) and [Cr(κ^3*NCN*-NCN^{CH2}-*i*Pr)(CH$_2$SiMe$_3$)] (**7**), respectively, in 72 and 68% isolated yields (Scheme 4). It has to be noted that complexes **6** and **7** can also be obtained directly from **2** via a one-pot reaction (see "Experimental"). Solution magnetic susceptibility measurements (Evans method, benzene) show that these complexes are also d^4-high-spin complexes with effective magnetic moments of 4.9(1) and 4.8(1) μ_B. A structural view of **6** is shown in Fig. 5 with selected bond distances and angles reported in the caption. The coordination geometry around the chromium center is best described by a slightly distorted square-planar arrangement with τ_4 and τ_4' values of 0.22 and 0.17, respectively. The C1–Cr1–C21 angle deviates from linearity being 173.29(5)°. The N1–Cr1–N2 angle is 154.99(4)°. The Cr–C$_{ipso}$ and the Cr–C$_{alkyl}$ bond distances are 2.043(1) and 2.249(1) Å, respectively.
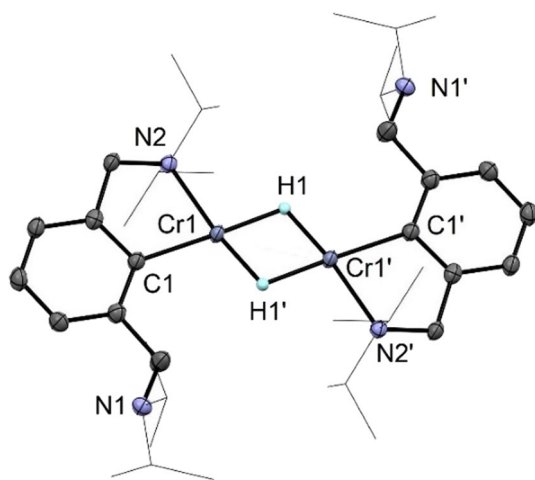
If a solution of lithiated N(C–Br)N^{CH2}-*i*Pr (**2**) is treated with anhydrous CrCl$_2$, followed by the addition of an excess of Na[HB(Et)$_3$] (3.5 equiv, 1 M solution in THF)

at −30 °C, after work up, the dimeric complex [Cr(κ^2*NC*-NCN^{CH2}-*i*Pr)(μ_2-H)]$_2$ (**8**) is obtained in 35% isolated yield (Scheme 5). A solution magnetic moment of μ_{eff} = 6.9(3) μ_B (Evans method, benzene) was determined which is consistent with eight unpaired electrons as expected for a high-spin d^4 configuration of the two metal centers. This also suggests that complex **8** contains no metal–metal bond (*vide infra*).

The molecular structure of **8** was unequivocally determined by X-ray crystallography. A structural view of **8** is given in Fig. 6 with selected bond distances and angles given in the caption. Complex **8** contains two μ_2-hydride ligands bridging the two Cr(II) centers. The distance of Cr1 to its image by inversion symmetry is 2.6941(6) Å which is in line with structurally related compounds found in literature [24–26, 29, 30]. Furthermore, **8** adopts an almost perfect square planar geometry around the chromium atoms with τ_4 and τ_4' values of 0.06 and 0.05, respectively.

The relevant orbitals obtained by DFT calculations for complex **8** are depicted in Fig. 7 and are consistent with two high-spin d^4 Cr(II) centers. Accordingly, the spin density of the molecule is located on the metal atoms as also shown in Fig. 7. The relevant Wiberg index (WI)[1] [31] for the Cr···Cr interaction is 0.15 indicating essentially no Cr–Cr metal bond. The two μ_2-hydrogen atoms are of a hydridic nature with NPA charges of −0.35.

Since a Cr(II) PCP alkyl complex was recently shown to be catalytically active for the hydrosilylation of ketones [22], we investigated the potential of the Cr(II) NCN alkyl complex **7** as a catalyst for this transformation. Complex **7** (1 mol% based on ketones) was reacted with both aromatic and aliphatic ketones and Si(OMe)$_3$H (2 equiv) in toluene (3 cm^3) at 25 °C. After workup with K$_2$CO$_3$/MeOH, all alcohols were isolated in yields up to 89% and were characterized by ^{1}H, ^{13}C{^{1}H}, and ^{19}F{^{1}H} NMR spectroscopy. These results are summarized in Table 1. The protocol tolerates halide (**9a**, **9b**), ether (**9c–9e**), and

---
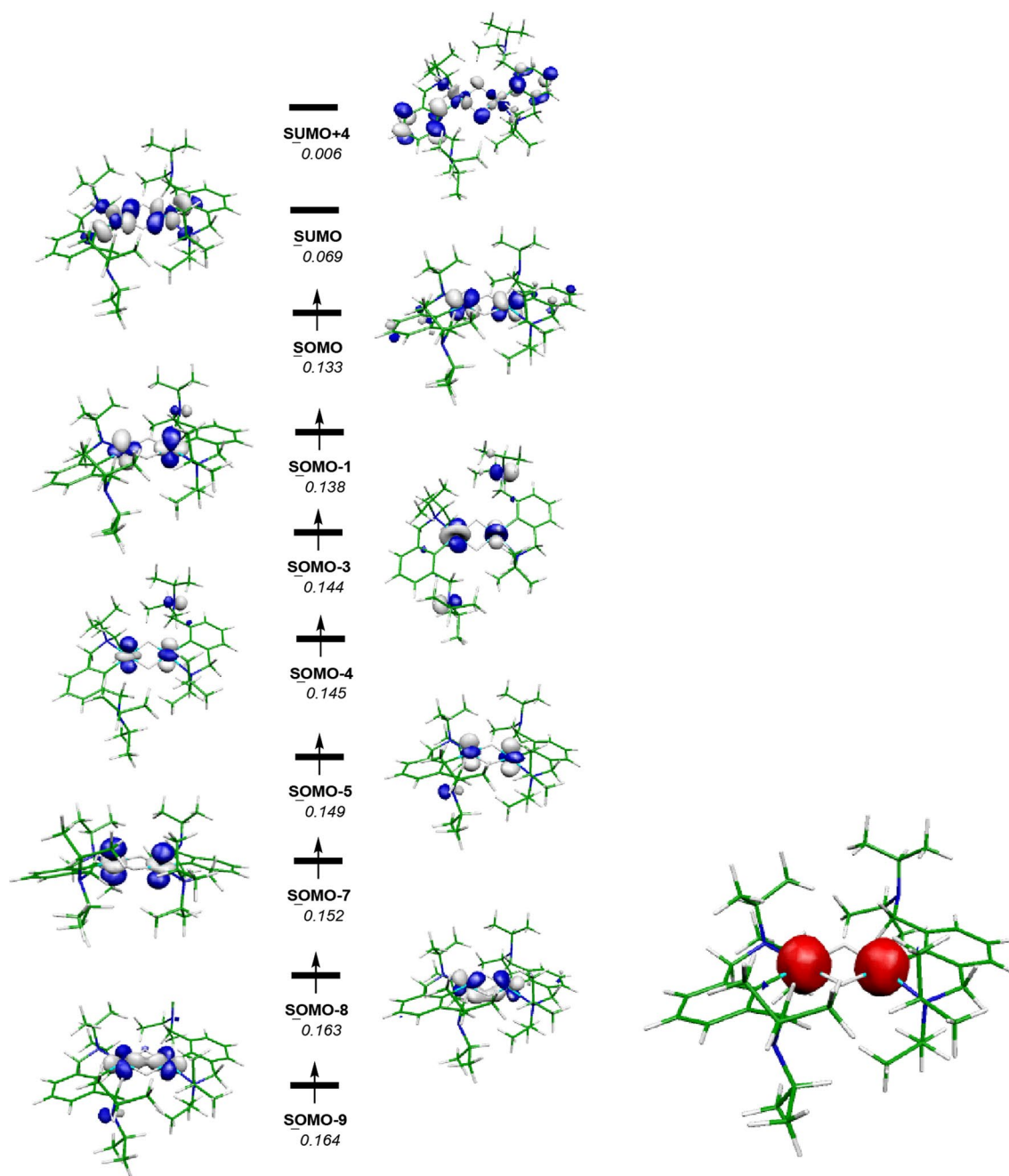
Fig. 7 Relevant orbitals (d-splitting, α-spin orbitals) and spin density for [Cr(κ²NC-NCN.^{CH2}-iPr)(μ$_2$-H)]$_2$ (**8**). Orbital energy values in hartrees (italics)

thiophene (**9i**) functionalities. Lower or no conversion was observed in the presence of amine (**9h**) and hydroxy (**9l**) groups. Likewise, aromatic ketones with substituents in the ortho positions resulted in no conversion (**9k**, **9m**). In sum, the catalytic activity of **7** is very similar to the analogous Cr(II) PCP pincer complex [Cr(κ³PCP-POCOP-iPr)-(CH$_2$SiMe$_3$)] [22].

Conclusion

In sum, we prepared and characterized several new Cr(II) and Cr(III) NCN pincer complexes with an arene backbone connected to amine donors NEt$_2$ and NiPr$_2$ via CH$_2$-linkers. The new complexes were typically prepared in a one-pot synthesis by reacting the in situ lithiated ligand precursors

Table 1 Hydrosilylation of ketones utilizing complex **7** as catalyst[a]

$$\underset{R^1 \quad R^2}{\overset{O}{\|}} \xrightarrow[\text{then } K_2CO_3/\text{MeOH}]{\begin{array}{c}\textbf{7} \text{ (1 mol\%), (MeO)}_3\text{SiH (2 equiv)}\\ \text{toluene, 25 °C, 1 h}\end{array}} \underset{R^1 \quad R^2}{\overset{OH}{|}}$$

9a 89%	**9b** 83%	**9c** 84%	**9d** 84%
9e 85%	**9f** 77%	**9g** 82%	**9h** 11%
	9i 88%	**9j** 76%	

not converted substrates

9k	**9l**	**9m**
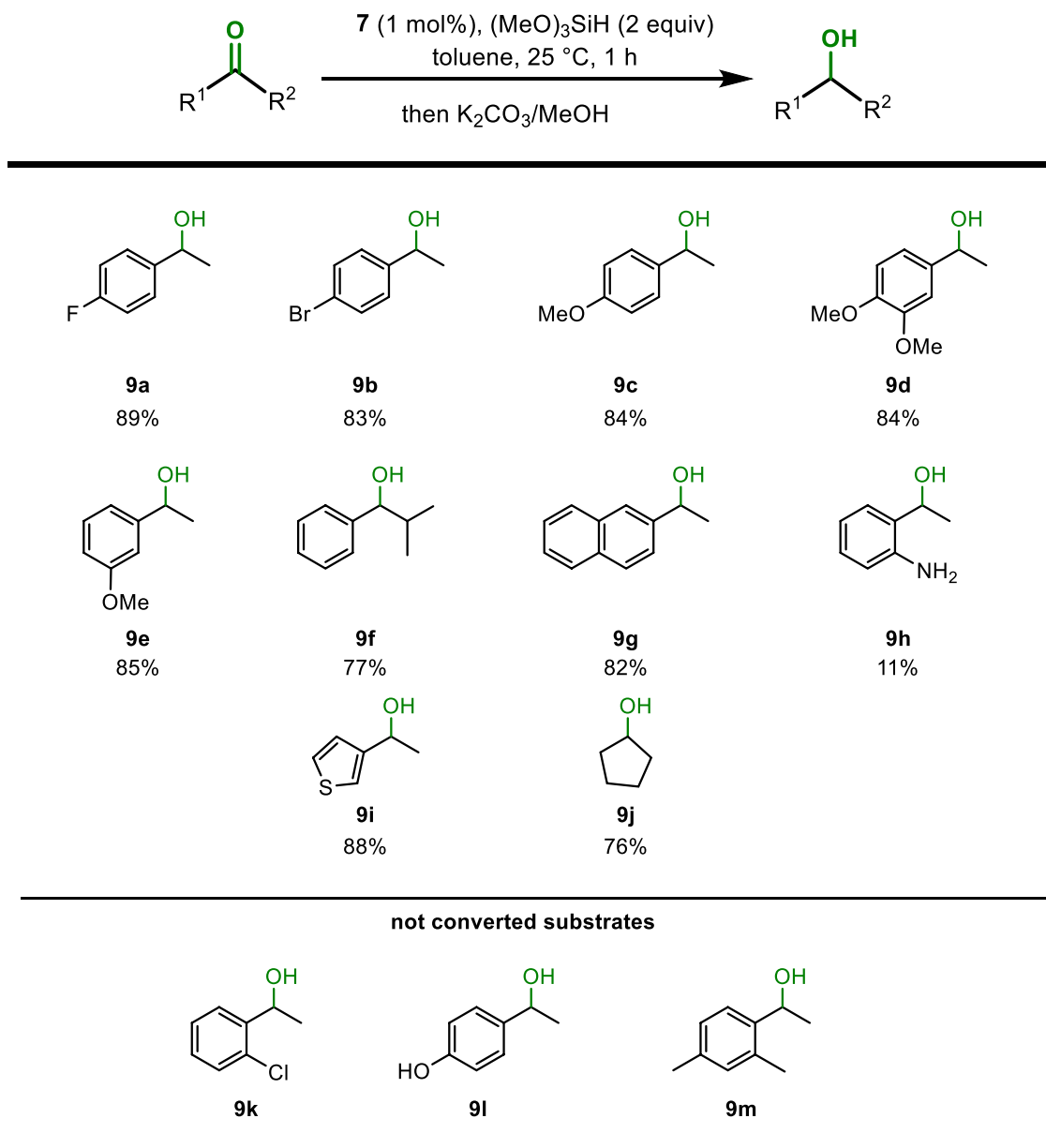
[a]Reaction conditions: 0.67 mmol ketone, 1.35 mmol Si(OMe)$_3$H (2 equiv), 1 mol% catalyst, 3 cm^3 toluene, 1 h, 25 °C. Isolated yields are reported

N(C–Br)N^{CH2}-Et (**1**) and N(C–Br)N^{CH2}-iPr (**2**) with the Cr(III) and Cr(II) precursors [CrCl$_3$(THF)$_3$] and anhydrous CrX$_2$ (X = Cl, Br), respectively. In the case of Cr(III), complex *trans*-[Cr(κ^3NCN-NCN^{CH2}-Et)(Cl)$_2$(THF)] (**3**) was obtained. In the case of Cr(II), the reaction of lithiated **2** with a suspension of anhydrous CrCl$_2$, complex [Cr(κ^2NC-NCN^{CH2}-iPr)$_2$] (**4**) featuring two NCN ligands bound in κ^2NC-fashion. If lithiated **2** is treated with a homogeneous solution of anhydrous CrX$_2$ (X = Cl, Br) complexes [Cr(κ^3NCN-NCN^{CH2}-iPr)X] (**5a**, **5b**) are obtained where the NCN ligand is coordinated in the typical meridional

κ^3NCN-mode. Treatment of **5a** with 1 equiv. of PhCH$_2$MgCl and LiCH$_2$SiMe$_3$ afforded the alkyl complex [Cr(κ^3NCN-NCN^{CH2}-iPr)(CH$_2$Ph)] (**6**) and [Cr(κ^3NCN-NCN^{CH2}-iPr)-(CH$_2$SiMe$_3$)] (**7**), respectively. If a solution of lithiated **2** is treated with CrCl$_2$ followed by the addition of an excess of Na[HB(Et)$_3$] the dimeric complex [Cr(κ^2NC-NCN^{CH2}-iPr)-(μ_2-H)]$_2$ (**8**) is formed bearing two μ_2-hydride ligands bridging the two Cr(II) centers. This complex displays a solution magnetic moment of μ_{eff} = 6.9(3) μ_B which is consistent with eight unpaired electrons as expected for a high-spin d^4 configuration of the two metal centers and no metal–metal

interaction. This finding was also confirmed by DFT calculations. Finally, the alkyl complex [Cr(κ^3NCN-NCN^{CH2}-iPr)(CH$_2$SiMe$_3$)] (**7**) turned out to be catalytically active for the hydrosilylation of aromatic and aliphatic ketones with Si(OMe)$_3$H at room temperature with a catalyst loading of 1 mol%. X-ray structures of all complexes are presented.

Experimental

All manipulations were performed under an inert atmosphere of argon by using Schlenk techniques or in an MBraun inert-gas glovebox. The solvents were purified according to standard procedures [32]. The deuterated solvents were purchased from Aldrich and dried over 3 Å molecular sieves. The ligands 1,1′-(2-bromo-1,3-phenylene)-bis-(*N,N*-diethylamine) (N(C–Br)N^{CH2}-Et) (**1**) and 1,1′-(2-bromo-1,3-phenylene)-bis-(*N,N*-diisopropylamine) (N(C–Br)N^{CH2}-iPr) (**2**) and anhydrous CrBr$_2$ were synthesized according to literature [33–35]. All other materials are known compounds and were used as obtained from commercial suppliers. ^{1}H, ^{13}C{^{1}H}, and ^{19}F{^{1}H} NMR spectra were recorded on Bruker AVANCE-250, AVANCE-400, and AVANCE-600 spectrometers. ^{1}H and ^{13}C{^{1}H} NMR spectra were referenced internally to residual protio-solvent and solvent resonances, respectively, and are reported relative to tetramethylsilane ($\delta = 0$ ppm). ^{19}F{^{1}H} NMR spectra were referenced externally to CFCl$_3$.

High-resolution-accurate mass spectra were recorded on a hybrid Maxis Qq-aoTOF mass spectrometer (Bruker Daltonics, Bremen, Germany) fitted with an ESI-source. Measured accurate mass data of the [M]$^+$ ions for confirming calculated elemental compositions were typically within 5 ppm accuracy. The mass calibration was done with a commercial mixture of perfluorinated trialkyl-triazines (ES Tuning Mix, Agilent Technologies, Santa Clara, CA, USA).

Electron Paramagnetic Resonance (EPR) spectra were recorded on an X-band Bruker Elexsys-II E500 CW-EPR spectrometer (Bruker Biospin GmbH, Rheinstetten, Germany) equipped with a high sensitivity cavity (SHQE1119) at 100 ± 1 K. The instrument parameters were set as follows: microwave frequency, 9.43 GHz; modulation frequency, 100 kHz, and microwave power, 15.9 mW. The spectra were analyzed using Xepr software and the Anisotropic SpinFit simulation program (both Bruker Biospin GmbH).

[2,3-Bis[(diethylamino)methyl]phenyl-*C,N,N′*](dichloro)(tetrahydrofuran)chromium(III), [Cr(κ^3NCN-NCN^{CH2}-Et)(Cl)$_2$(THF)] (3, C$_{20}$H$_{35}$Cl$_2$CrN$_2$O) A solution of (N(C–Br)N^{CH2}-Et) (**1**, 400 mg, 1.23 mmol) in THF (13 cm^3) was cooled to -90 °C. After stirring for 10 min, *n*-BuLi (1.52 cm^3, 1.6 M in hexanes, 2.46 mmol) was added dropwise via a syringe and the light-yellow solution was stirred at -90 °C for 2.5 h. After

warming up to -30 °C, [CrCl$_3$(THF)$_3$] (460 mg, 1.23 mmol) was added portion-wise under stirring resulting in the formation of a dark green solution. The solution was allowed to warm to room temperature and was stirred for 12 h. After removal of the solvent under reduced pressure, the residue dissolved in toluene (7 cm^3) and filtered through celite. After removal of the toluene, the residue was washed three times with *n*-pentane (3 × 10 cm^3). Drying under reduced pressure yielded a light-purple solid. Yield: 340 mg (63%). Dark green crystals suitable for X-ray crystallography were obtained by slow diffusion of *n*-pentane into a saturated THF solution of **3**. $\mu_{eff} = 3.7(2)$ μ_B (Evans method, THF); HR-MS (ESI$^+$, THF): *m/z* calcd for C$_{16}$H$_{27}$Cl$_2$CrN$_2$ ([M-THF+H]$^+$) 370.1029, found 370.1031.

Bis-[2,3-bis[(diisopropylamino)methyl]phenyl-*C,N,N′*]-chromium(II), [Cr(κ^2NC-NCN^{CH2}-*i*Pr)$_2$] (4, C$_{40}$H$_{70}$CrN$_4$) A solution of (N(C–Br)N^{CH2}-*i*Pr) (**2**, 100 mg, 0.26 mmol) in THF (7 cm^3) was cooled to -90 °C. After stirring at that temperature for 10 min, *n*-BuLi (0.18 cm^3, 1.6 M, 0.30 mmol) was added dropwise via a syringe. A suspension of anhydrous CrCl$_2$ (38 mg, 0.30 mmol) in THF (4 cm^3) was added in a dropwise fashion at -20 °C. After the addition was completed, all volatiles were removed under reduced pressure and the residue was extracted with *n*-pentane (6 cm^3) and filtered through a syringe filter (PTFE, 0.2 µm). The solvent was removed under vacuum yielding a dark blue solid. Yield: 45 mg (37%). Blue crystals suitable for X-ray crystallography were obtained by cooling a saturated *n*-pentane solution of **4** to -30 °C. $\mu_{eff} = 4.7(3)$ μ_B (Evans method, benzene). HR-MS spectra could not be obtained due to the highly air-sensitive nature of the compound.

[2,3-Bis[(diisopropylamino)methyl]phenyl-*C,N,N′*]-(chloro)chromium(II), [Cr(κ^3NCN-NCN^{CH2}-*i*Pr)Cl] (5a, C$_{20}$H$_{35}$ClCrN$_2$) Anhydrous CrCl$_2$ (38 mg, 0.30 mmol) was suspended in THF (15 cm^3). The suspension was exposed to ultrasonic irradiation for 1 h to form a light-blue clear solution. The ligand (N(C–Br)N^{CH2}-*i*Pr) (**2**) (100 mg, 0.26 mmol) was dissolved in THF (5 cm^3) and subsequently cooled to -90 °C. After stirring at that temperature for 10 min, *n*-BuLi (0.18 cm^3, 1.6 M, 0.30 mmol) was added dropwise via a syringe. The orange solution was stirred for 30 min before it was allowed to warm to 0° C while stirring for another hour. The lithiated intermediate was added in a dropwise fashion to the THF solution of CrCl$_2$ via a syringe. The solution was allowed to stir for 15 min at room temperature before all volatiles were evaporated under vacuum. The residue was extracted into *n*-pentane (7 cm^3) and filtered through a syringe filter (PTFE, 0.2 µm). The volume of the filtrate was reduced to about 1.5 cm^3 and stored at -30 °C to afford **5** as dark purple crystalline plates suitable for X-ray diffraction analysis. Yield: 75 mg (73%);

$\mu_{\text{eff}} = 4.8(2)\ \mu_B$ (Evans method, benzene). HR-MS spectra could not be achieved due to the highly air-sensitive nature of the compound.

[2,3-Bis[(diisopropylamino)methyl]phenyl-*C,N,N′*]-(bromo)chromium(II), [Cr(κ³*NCN*-NCN^{CH2}-*i*Pr)Br (5b, C₂₀H₃₅BrCrN₂) Complex **5b** was prepared analogously to complex **5a** utilizing anhydrous CrBr₂ (58 mg, 0.30 mmol) and N(C–Br)N^{CH2}-iPr (**2**) (100 mg, 0.26 mmol) as starting materials. Yield: 85.2 mg (75%); $\mu_{\text{eff}} = 4.7(2)\ \mu_B$ (Evans method, benzene). HR-MS spectra could not be obtained due to the highly air-sensitive nature of the compound.

[2,3-Bis[(diisopropylamino)methyl]phenyl-*C,N,N′*](phenyl)-(methyl)) chromium(II), [Cr(κ³*NCN*-NCN^{CH2}-*i*Pr)(CH₂Ph)](6, C₂₇H₄₂CrN₂) *Method A.* A suspension of anhydrous CrCl₂ (38 mg, 0.30 mmol) in THF (15 cm³) was placed in an ultrasonic bath for 1 h whereupon the suspension turned into light blue solution. (N(C–Br)N^{CH2}-*i*Pr) (**2**, 100 mg, 0.26 mmol) was dissolved in THF (5 cm³) and subsequently cooled to −90 °C. After stirring for 10 min, *n*-BuLi (0.18 cm³, 1.6 M, 0.30 mmol) was added dropwise and the solution was stirred for additional 30 min. The solution was allowed to warm to 0 °C and was stirred for 1 h. The lithiated intermediate was then added in a dropwise fashion to THF solution of CrCl₂ and a dark-colored solution was formed immediately. The solution was stirred for 15 min at room temperature and all volatiles were then evaporated under vacuum. The residue was dissolved in benzene and the solution was filtered through a syringe filter (PTFE, 0.2 μm). A solution of PhCH₂MgCl (0.1 cm³, 1 M in THF) was then added and the suspension was stirred for 1.5 h. All volatiles were removed under reduced pressure. The remaining residue was extracted with *n*-pentane (3 cm³) and filtered through syringe filter (PTFE, 0.2 μm). Evaporation of the solvent afforded **6** as a dark brown solid. Cooling of a saturated *n*-pentane solution of 6 to −30° C yielded crystals suitable for X-ray diffraction. Yield: 81 mg (72%); $\mu_{\text{eff}} = 4.9(1)\ \mu_B$ (Evans method, benzene).

Method B. Complex **6** was also obtained by reacting isolated **5a** (50 mg, 0.12 mmol) in benzene (2 cm³) with PhCH₂MgCl (0.14 cm³, 1 M in THF) and stirring for 1.5 h at room temperature. After evaporating the solvent under reduced pressure, redissolving the residue in *n*-pentane (2 cm³) and subsequent filtration (syringe filter PTFE, 0.2 μm) and removal of the solvent, **6** could be isolated as a dark brown solid. Yield: 41 mg (72%). HR-MS spectra could not be achieved due to the highly air-sensitive nature of the compound.

[2,3-Bis[(diisopropylamino)methyl]phenyl-*C,N,N′*](tri-methylsilane)(methyl)chromium(II), [Cr(κ³*NCN*-NCN^{CH2}-*i*Pr)-(CH₂SiMe₃)] (7, C₂₄H₄₆CrN₂Si) *Method A.* Complex **7** was prepared in an analogous fashion to **6** utilizing LiCH₂TMS (0.28 cm³, 0.28 mmol, 1 M in *n*-pentane). Complex **7** was obtained as a dark brown solid. Yield: 76 mg (68%); $\mu_{\text{eff}} = 4.8(1)\ \mu_B$ (Evans method, benzene).

Method B. A solution of Complex **5a** (50 mg, 0.12 mmol) in benzene (2 cm³) was treated with LiCH₂TMS (0.13 cm³, 0.28 mmol, 1 M in *n*-pentane) and stirring for 1.5 h at room temperature. After evaporation of the solvent, redissolving the residue in *n*-pentane (2 cm³) and subsequent filtration (syringe filter PTFE, 0.2 μm) and removal of the solvent, **7** could be isolated as a dark brown solid. Yield: 39 mg (69%). HR-MS spectra could not be obtained due to the highly air-sensitive nature of the compound.

Bis-[2,3-bis[(diisopropylamino)methyl]phenyl-*C,N,N′*])-(μ₂-hydrido)chromium(II)], [Cr(κ²*NC*-NCN^{CH2}-*i*Pr)(μ₂-H)]₂ (8, C₄₀H₇₂Cr₂N₄) A suspension of anhydrous CrCl₂ (38 mg, 0.30 mmol) in THF (15 cm³) was placed in an ultrasonic bath for 1 h, whereupon a light blue solution was obtained. The ligand precursor N(C–Br)N^{CH2}-*i*Pr (**2**, 100 mg, 0.26 mmol) was dissolved in THF (5 cm³) and cooled to −90 °C. After stirring for 10 min, *n*-BuLi (0.18 cm³, 1.6 M, 0.30 mmol) was added dropwise via a syringe and the orange solution was further stirred for 30 min and then allowed to warm to 0 °C and stirred for an additional 1 h. The solution containing lithiated N(C–Br)N^{CH2}-*i*Pr (**2**) was added dropwise to the THF-solution of anhydrous CrCl₂ whereupon the solution became dark purple. The solution was allowed to stir for 15 min at room temperature before all volatiles were evaporated under vacuum. The residue was dissolved in benzene and filtered through a syringe filter (PTFE, 0.2 μm) and volatiles were evaporated under reduced pressure. The residue was dissolved in precooled THF (−30 °C, 3 cm³) and treated with NaHBEt₃ (0.91 cm³, 0.91 mmol, 1 M in THF) and stirred for 30 min. After removal of the solvent, the remaining residue was redissolved in *n*-pentane (10 cm³), filtered through a syringe filter (PTFE, 0.2 μm) and the volume of the solution was reduced to approximately 1 cm³. Storage of the light brown solution at -30 °C for 12 h led to the formation of bright orange crystals. Yield: 64 mg (35%); $\mu_{\text{eff}} = 6.9(3)\ \mu_B$ (Evans method, benzene-d_6); HR-MS (ESI⁺, THF): *m/z* calcd for C₄₀H₇₂Cr₂N₄ ([M-C₂₀H₃₆CrN₂]⁺) 356.2279, found 356.2278.

General procedure for the hydrosilylation of ketones

To a solution of the substrate (0.67 mmol, 1 equiv.) and HSi(OMe)₃ (174 mm³, 1.35 mmol, 2 equiv) in toluene (3 cm³) complex **7** was added (3 mg, 6.7 μmol, 1 mol%) causing an immediate color change. The mixture was stirred at room temperature for 1 h and then a saturated methanolic K₂CO₃ solution (3 cm³) was added to the mixture. After

stirring for 5 h volatiles were evaporated under reduced pressure. The residue was dissolved in CH_2Cl_2 (6 cm^3) and filtered through a short plug of silica. After evaporation of the solvent, the reaction products were analyzed by the means of ^1H, ^{13}C {^1H}, and ^{19}F{^1H} NMR spectroscopy.

X-ray structure determination

X-ray diffraction data of **3**, **4**, **5a** (CCDC 2285377–2285379) and **8** (CCDC 2285381) were collected at $T = 100$ K in a dry stream of nitrogen on a Bruker Kappa APEX II diffractometer system using graphite-monochromatized Mo-$K\alpha$ radiation ($\lambda = 0.71073$ Å) and fine sliced φ- and ω-scans. Data were reduced to intensity values with SAINT and an absorption correction was applied with the multi-scan approach implemented in SADABS [36]. Data of **6** (CCDC 2285380) were collected at $T = 100$ K on a Rigaku XtaLAB Synergy, Dualflex diffractometer system equipped with a HyPix hybrid photon counting detector using Cu-$K\alpha$ radiation ($\lambda = 1.54184$ Å). Data were reduced and an absorption correction applied using the multi-scan approach with the CrysAlisPro software [37]. The structures were solved by the dual-space approach implemented in SHELXT [38] and refined against F^2 with SHELXL [39]. Non-hydrogen atoms were refined with anisotropic displacement parameters. H atoms attached to C were placed in calculated positions and thereafter refined as riding on the parent atoms. The positions of the hydride hydrogens in **8** were freely refined. The halogenide ligands in **3** and **5a** were modelled as occupationally disordered Cl/Br sites with the total occupation of each sit e constrained to 1. Molecular graphics were generated with the program MERCURY [40].

Computational details

The computational results presented have been achieved in part using the Vienna Scientific Cluster (VSC). Calculations were performed using the GAUSSIAN 09 software package [41] and the OPBE [42–45] functional without symmetry constraints, the Stuttgart/Dresden ECP (SDD) basis set [46–48] to describe the electrons of the chromium atom and a standard 6-31G** basis for all other atoms as already previously described [49–53]. Population analysis (NPA) [54–61] and the resulting Wiberg indices [31] were used to study the electronic structure and bonding of the optimized species. The NPA analysis was performed with the NBO 5.0 program [62]. The α-spin orbitals and spin density drawings (Fig. 7) were obtained with the program Molekel [63].

References

1. Gossage RA, van de Kuil LA, van Koten G (1998) Acc Chem Res 31:423
2. Albrecht M, van Koten G (2001) Angew Chem Int Ed 40:3750
3. van der Boom ME, Milstein D (2003) Chem Rev 103:1759
4. Liang LC (2006) Coord Chem Rev 250:1152
5. Morales-Morales D, Jensen CM (2007) The chemistry of pincer compounds. Elsevier, Amsterdam
6. Nishiyama H (2007) Chem Soc Rev 36:1133
7. Benito-Garagorri D, Kirchner K (2008) Acc Chem Res 41:201
8. Choi J, MacArthur AHR, Brookhart M, Goldman AS (2011) Chem Rev 111:1761
9. Selander N, Szabo KJ (2011) Chem Rev 111:2048
10. Schneider S, Meiners J, Askevold B (2012) Eur J Inorg Chem 2012:412
11. van Koten G, Milstein D (2013) organometallic pincer chemistry. Springer, Berlin
12. Murugesan S, Kirchner K (2016) Dalton Trans 45:416
13. Grove DM, van Koten G, Ubbels HJC, Zoet R (1984) Organometallics 3:1003
14. Slagt MQ, van Zwieten DAP, Moerkerk AJCM, Klein Gebbink RJM, van Koten G (2004) Coord Chem Rev 248:2275
15. Back S, Gossage RA, Lang H, van Koten G (2000) Eur J Inorg Chem 1457
16. Rodriguez G, Lutz M, Spek AL, van Koten G (2002) Chem Eur J 8:45
17. van der Zeijden AAH, van Koten G, Luijk R, Vrieze K, Slob C, Krabbendam H, Spek AL (1988) Inorg Chem 27:1014
18. Schimmelpfennig U, Simmering RZ, Schleinitz KD, Stößer R, Wenschuh E (1993) Z Anorg Allg Chem 619:1931
19. Adams JJ, Arulsamy N, Roddick DM (2012) Organometallics 31:1439
20. Pecak J, Eder W, Tomsu G, Pignitter M, Kirchner K (2021) Eur J Inorg Chem 41:4280

21. Himmelbauer D, Mastalir M, Stöger B, Veiros LF, Kirchner K (2018) Organometallics 37:3631
22. Himmelbauer D, Stöger B, Pignitter M, Veiros LF, Kirchner K (2019) Organometallics 38:4669
23. Eder W, Stöger B, Kirchner K (2019) Monatsh Chem 150:1235
24. Ott JC, Isak D, Melder JJ, Wadepohl H, Gade LH (2020) Inorg Chem 59:14526
25. Schiwek CH, Vasilenko V, Wadepohl H, Gade LH (2018) Chem Commun 54:9139
26. Liu Z, Gao W, Liu X, Luo X, Cui D, Mu Y (2011) Organometallics 30:752
27. Sur SK (1989) J Magn Reson 82:169
28. Addison AW, Rao TN, Reedijk J, van Rijn J, Verschoor GC (1984) J Chem Soc Dalton Trans 1349
29. Fryzuk MD, Leznoff DB, Rettig SJ, Thompson RC (1994) Inorg Chem 33:5528
30. MacAdams LA, Buffone GP, Incarvito CD, Golen JA, Rheingold AL, Theopold KH (2003) Chem Commun 3:1164
31. Wiberg KB (1968) Tetrahedron 24:1083
32. Perrin DD, Armarego WLF (1988) Purification of laboratory chemicals, 3rd edn. Pergamon, New York
33. van Beek JAM, van Koten G, Dekker GPCM, Wissing E, Zoutberg MC, Stam CH (1990) J Organomet Chem 394:659
34. Bibal C, Mazières S, Gornitzka H, Couret C (2002) Polyhedron 21:2827
35. Kurogi T, Irifune K, Takai K (2021) Chem Sci 12:14281
36. Bruker computer programs (2020) APEX3, SAINT, SADABS. Bruker AXS Inc., Madison
37. Rigaku Oxford Diffraction (2022) CrysAlisPro software system version 1.171.42.69a. Rigaku Corporation, Wrocław
38. Sheldrick GM (2015) Acta Crystallogr A 71:3
39. Sheldrick GM (2015) Acta Crystallogr C 71:3
40. Macrae CF, Edgington PR, McCabe P, Pidcock E, Shields GP, Taylor R, Towler M, van de Streek J (2006) J Appl Cryst 39:453
41. Frisch MJ, Trucks GW, Schlegel HB, Scuseria GE, Robb MA, Cheeseman Jr, Scalmani G, Barone V, Mennucci B, Petersson GA, Nakatsuji H, Caricato M, Li X, Hratchian HP, Izmaylov AF, Bloino J, Zheng G, Sonnenberg JL, Hada M, Ehara M, Toyota K, Fukuda R, Hasegawa J, Ishida M, Nakajima T, Honda Y, Kitao O, Nakai H, Vreven T, Montgomery JA Jr, Peralta JE, Ogliaro F, Bearpark M, Heyd JJ, Brothers E, Kudin KN, Staroverov VN, Kobayashi R, Normand J, Raghavachari K, Rendell A, Burant JC, Iyengar SS, Tomasi J, Cossi M, Rega N, Millam JM, Klene M, Knox JE, Cross JB, Bakken V, Adamo C, Jaramillo J, Gomperts R, Stratmann RE, Yazyev O, Austin AJ, Cammi R, Pomelli C, Ochterski JW, Martin RL, Morokuma K, Zakrzewski VG, Voth GA, Salvador P, Dannenberg JJ, Dapprich S, Daniels AD, Farkas Ö, Foresman JB, Ortiz JV, Cioslowski J, Fox DJ (2009) Gaussian 09, revision A0.2. Gaussian Inc., Wallingford
42. Handy NC, Cohen AJ (2001) Mol Phys 99:403
43. Hoe WM, Cohen A, Handy NC (2001) Chem Phys Lett 341:319
44. Perdew JP, Burke K, Ernzerhof M (1997) Phys Rev Lett 78:1396
45. Perdew JP, Burke K, Ernzerhof M (1996) Phys Rev Lett 77:3865
46. Haeusermann U, Dolg M, Stoll H, Preuss H, Schwerdtfeger P, Pitzer RM (1993) Mol Phys 78:1211
47. Kuechle W, Dolg M, Stoll H, Preuss H (1994) J Chem Phys 100:7535
48. Leininger T, Nicklass A, Stoll H, Dolg M, Schwerdtfeger P (1996) J Chem Phys 105:1052
49. Ditchfield R, Hehre WJ, Pople JA (1971) J Chem Phys 54:724
50. Hehre WJ, Ditchfield R, Pople JA (1972) J Chem Phys 56:2257
51. Hariharan PC, Pople JA (1974) Mol Phys 27:209
52. Gordon MS (1980) Chem Phys Lett 76:163
53. Hariharan PC, Pople JA (1973) Theor Chim Acta 28:213
54. Carpenter JE, Weinhold F (1988) J Mol Struct (Theochem) 169:41
55. Carpenter JE (1987) PhD thesis. University of Wisconsin, Madison, WI
56. Foster JP, Weinhold F (1980) J Am Chem Soc 102:7211
57. Reed AE, Weinhold F (1983) J Chem Phys 78:4066
58. Reed AE, Weinhold F (1985) J Chem Phys 83:1736
59. Reed AE, Weinstock RB, Weinhold F (1985) J Chem Phys 83:735
60. Reed AE, Curtiss LA, Weinhold F (1988) Chem Rev 88:899
61. Weinhold F, Carpenter JE (1988) The structure of small molecules and ions. Plenum, New York, p 227
62. Glendening ED, Badenhoop JK, Reed AE, Carpenter JE, Bohmann JA, Morales CM, Weinhold F (2001) NBO 5.0. Theoretical Chemistry Institute, University of Wisconsin, Madison
63. Portmann S, Lüthi HP (2000) Chimia 54:766